

Design of a Robot's Hand with Two 3-Axis Force Sensor for Grasping an Unknown Object

Gab-Soon Kim^{1, #}

¹ ERI, School of Control and Instrumentation Engineering, Gyeongsang National University, Jinju, South Korea

ABSTRACT

This paper describes the design of a robot's hand with two fingers for stably grasping an unknown object, and the development of a 3-axis force sensor for which is necessary to constructing the robot's fingers. In order to safely grasp an unknown object using the robot's fingers, they should measure the forces in the gripping and in the gravity directions, and control the measured forces. The 3-axis force sensor should be used for accurately measuring the weight of an unknown object in the gravity direction. Thus, in this paper, the robot's hand with two fingers for stably grasping an unknown object is designed, and the 3-axis force sensor is newly modeled and fabricated using several parallel-plate beams.

Key Words : Robot's hand, Robot's finger, 3-axis force sensor, Parallel-plate beam, Rated strain, Interference error, Strain gage

1. Introduction

Robot's gripper has widely been studied recently. M. Ceccarelli, et al.¹ made the robot's finger with a force sensor for only measuring the force in the grasping direction, and performed the position and the force control for gripping an unknown object. D. Castro, et al.² manufactured jaw gripper using the Fx force sensor, and carried out the force control using it. N. S. Tlale, et al.³ fabricated the intelligent gripper with a contact sensor and a control circuit. Carlos M. Valente et al.⁴ designed a three-finger gripper with the vision system which could accurately found the position of an object. And, D.J. O'Brien, et al.⁵ fabricated the gripper with the finger that could measure the force only in the grasping direction.

However, the above grippers can not stably grasp an unknown object, because they do not measure the force Fx in the x-direction (the force in the grasping direction), the force Fy in the y-direction and the force Fz in the z-

direction simultaneously. In order to stably grasp an unknown object, the two robot's fingers should measure the forces in the grasping direction as well as in the gravity direction, and perform the force control based on the measured forces.

Therefore, the robot's hand should be composed of the fingers with a 3-axis force sensor for measuring the forces Fx, Fy and Fz simultaneously. The accuracy of a 3-axis force sensor signifies the interference errors because the interference error is larger than that from the non-linearity or the repeatability⁶⁻⁸. In order to make the 3-axis force sensor accurately, the sensing elements of the sensor should be designed to minimize the interference errors, and strain distributions on the sensing elements should also be analyzed.⁹⁻¹³

Thus, in this paper, the robot's hand with two fingers for stably grasping an unknown object is designed, and the 3-axis force sensor for measuring the forces Fx, Fy, and Fz simultaneously is developed. The 3-axis force sensor is newly modeled using several parallel-plate beams, the equations for calculating the strains on each plate beam under forces are derived. The reliability of the derived equations is verified by performing a FEM (finite

Corresponding Author :
Email : gskim@nongae.gsnu.ac.kr
Tel. +82-55-751-5372

element method) analysis. And, the modeled 3-axis force sensor is designed, fabricated and evaluated. Also, the equations for calculating the weight of an unknown object using the robot's hand with the 3-axis force sensor are derived.

2. Design of robot's finger

2.1 Robot's hand

Fig. 1 shows the robot's hand with two fingers. Each consists of two links, four motors and a block. The robot's hand with the 3-axis force sensor for measuring the forces F_x , F_y and F_z simultaneously can stably grip an unknown object by carrying out the position and force control. That is, the robot's hand with the 3-axis force sensor does not break or drop an unknown object, and can accurately perform next action. Each sensor measures the force in each direction and the force in the gravity direction is calculated by using the measured forces. Also, the F_x sensor measures the force in the grasping direction.

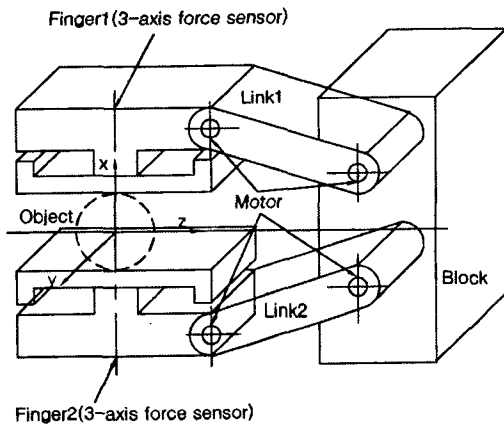


Fig. 1 Robot's hand with the two fingers

Fig. 2 shows two robot's fingers and an unknown object in two different Cartesian coordinates. Cartesian coordinates of two robot's fingers and the unknown object are represented in x, y, z and x', y', z' frames, respectively.

The force vector \vec{F}' (the weight vector of an unknown object) in x', y', z' frame can be expressed as

$$\vec{F}' = F'_x \vec{a}'_x + F'_y \vec{a}'_y + F'_z \vec{a}'_z \quad (1)$$

where F'_x, F'_y, F'_z are the force components in each x', y', z' direction, respectively, $\vec{a}'_x, \vec{a}'_y, \vec{a}'_z$ are the unit vectors in each x', y', z' direction, respectively. Finally, the force vector $\vec{F}' = -mg\vec{a}'_x$, that is, $F'_x = -mg$, where m is mass of an unknown object and g is the gravity acceleration.

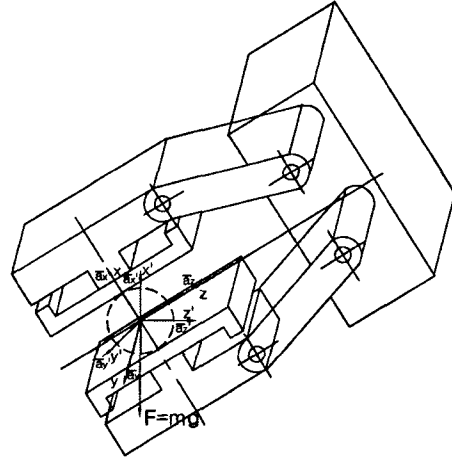


Fig. 2 Two robot's fingers and an unknown object in different Cartesian coordinates

The force vector \vec{F} of robot's finger in x, y, z frame can be written as

$$\vec{F} = F_x \vec{a}_x + F_y \vec{a}_y + F_z \vec{a}_z = F_k \vec{a}_k \quad (2)$$

where F_x, F_y, F_z are the force components in x, y, z direction, respectively, $\vec{a}_x, \vec{a}_y, \vec{a}_z$ are the unit vectors in x, y, z direction, respectively, F_k is the magnitude of the force applied to the 3-axis force sensor and \vec{a}_k is the unit vector in the force direction. The magnitude of the force applied F_k can be represented as

$$F_k = \sqrt{F_x^2 + F_y^2 + F_z^2} \quad (3)$$

Because the 3-axis sensor measures the weight of an unknown object, the force vector \vec{F} can be expressed as

$$\vec{F} = F_k \vec{a}_k = -(\sqrt{F_x^2 + F_y^2 + F_z^2}) \vec{a}'_x = -mg \vec{a}'_x \quad (4)$$

Thus, the weight of an unknown object mg can be calculated by using equation (4). The force F_x is the

measured value from the F_x sensor, whereas the forces F_y and F_z are from the F_y and F_z sensor.

2.2 Modeling of sensing elements of finger

Fig. 3 shows the finger with 3-axis force sensor that measures the forces F_x , F_y and F_z , simultaneously. As shown in Fig. 3, robot's finger is composed of a 3-axis force sensor, two contact plates and a finger frame. The 3-axis force sensor consists of five parallel-plate beams (PPBs). The sensing elements for measuring the forces F_x , F_y and F_z are PPB 1 and 2, PPB 3 and 4, and PPB5, respectively. The PPB1, PPB2, PPB3 and PPB4 is composed of two plate beams of the same size (thickness and length are t_1 , l_1). They are symmetrical in the respect vertical center axis. Also, the PPB5 is composed of two plate beams of the same size (thickness and length are t_2 , l_2). The contact plate is contacted with an unknown object and fixed with the center block of the 3-axis force sensor. The finger frame is fixed with both end of the 3-axis force sensor and transfers the torque from motor to the sensor. The strains on each plate beam are used to design each force sensor. It is thus necessary to analyze the strains on the plate beams through the theoretical analysis and the finite element method.

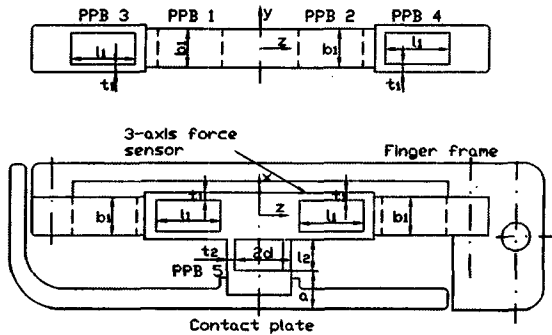


Fig. 3 The sensing elements of the robot's finger (3-axis force sensor)

2.3 Theoretical analysis of sensing elements

In order to analyze the strains on the PPB 1, PPB 2, PPB 3, and PPB 4, the equations need to be derived only for analyzing the strains of the PPB 3 under the force F_y , because the PPB 1, PPB 2, PPB 3, and PPB 4 consist of the two plate beams of the same size. Also, The equations for analyzing the strains of the PPB 5 are derived under the force F_z . Each size of the sensing

elements can be determined by using the derived equations.

2.3.1 Under the applied force F_y

Fig. 4 shows the diagram for analyzing the strains on each plate beam when the force F_y is applied along the y-direction central line between the PPB 3 and PPB 4. The PPB 3 and PPB 4 are symmetrical with respect to the center axis along which the force F_y is applied. The plate beam 1 and beam 2 (PPB 3), the plate beam 3 and beam 4 (PPB 4) are symmetrical with respect to the horizontal center axis. The equations for analyzing the strains of plate beam 1 can thus be applied to the plate beam 2, the plate beam 3 and the plate beam 4. Also, the equations for force F_y can be used those for force F_x .

The force F_{Fyy} can be expressed as

$$F_{Fyy} = \frac{F_y}{4} \quad (5)$$

where F_{Fyy} is the y-direction force generated to plate beam due to force F_y .

The moment equilibrium condition at point O ($\sum M_o=0$) can be written as

$$2M_{Fyx} - F_{Fyy}l_1 = 0 \quad (6)$$

where M_{Fyx} is the x-direction moment generated to plate beam due to force F_y .

By substituting the equation (5) into (6), the moment M_{Fyx} can be derived as

$$M_{Fyx} = \frac{F_y l_1}{8} \quad (7)$$

The moment M_z at an arbitrary point z leads to

$$M_z = \frac{F_y}{4} \left(z - \frac{l_1}{2} \right) \quad (8)$$

The equations ε_{Fy-U} and ε_{Fy-L} for calculating the strains on the upper and lower surfaces of the plate beam 1 can be derived by substituting the equation (8) into the bending strain equation $\varepsilon = M_z / EZ_{1p}$, as

$$\varepsilon_{Fy-U} = \frac{F_y}{4EZ_{1p}} \left(z - \frac{l_1}{2} \right) \quad (9-a)$$

$$\varepsilon_{Fy-L} = \frac{F_y}{4EZ_{1p}} \left(\frac{l_1}{2} - z \right) \quad (9-b)$$

where E is modulus of longitudinal elasticity, Z_{1p} is polar moment of inertia.

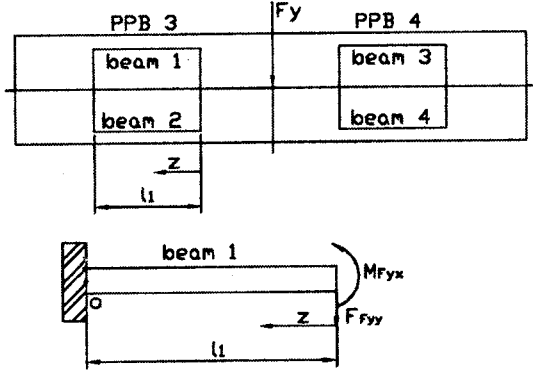


Fig. 4 Free body diagram of plate beams for a 3-axis force sensor under the force F_y

2.3.2 Under the force F_z

Fig. 5 shows the diagram for analyzing the strains on each plate beam under the force F_z . The plate beams 5 and 6 (PPB 5) are symmetrical with respect to the horizontal center axis. Thus, the equations for analyzing the strains on plate beam 5 can be used for the plate beam 6.

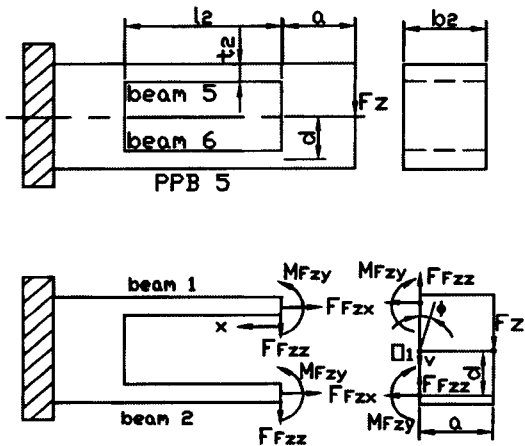


Fig. 5 Free body diagram of plate beams for a 3-axis force sensor under the force F_z

In the plate beam 5 and 6, the force F_{Fzz} , F_{Fzx} , and the moment M_{Fzy} can be expressed as

$$F_{Fzz} = \frac{12EI_2}{l_2^3} \left[v + \left(a + \frac{l_2}{2} \right) \phi \right] \quad (10)$$

$$F_{Fzx} = \frac{A_2Ed\phi}{l_2} \quad (11)$$

$$M_{Fzy} = \frac{12EI_2}{l_2^2} \left[\frac{v}{2} + \left(\frac{a}{2} + \frac{l_2}{3} \right) \phi \right] \quad (12)$$

where F_{Fzz} is the z-direction force acting to plate beam due to force F_z , F_{Fzx} is the x-direction force generated to plate beam due to force F_z , and M_{Fzy} is the y-direction moment generated to plate beam due to force F_z .

The moment equilibrium condition at the point O_1 , $\Sigma M_{O1} = 0$, can be written as

$$aF_z - 2dF_{Fzx} + 2M_{Fzy} = 0 \quad (13)$$

By substituting the equations (10)~(12) into (13), the rotation angle ϕ , and the vertical displacement v can be derived as

$$\phi = \frac{(2a + l_2)F_z}{\frac{48EI_2}{l_2^2} \left(\frac{3}{2}a + \frac{2}{3}l_2 \right) + \frac{4A_2Ed^2}{l_2}} \quad (14)$$

$$v = \frac{F_z - \frac{24EI_2}{l_2^2} \left(a + \frac{l_2}{2} \right) \phi}{\frac{24EI_2}{l_2^2}} \quad (15)$$

The moment M_x at arbitrary point x leads to

$$M_x = \frac{12E_2I_2x}{l_2^3} \left[v + \left(a + \frac{l_2}{2} \right) \phi \right] - \frac{12EI_2}{l_2^2} \left[\frac{v}{2} + \left(\frac{a}{2} + \frac{l_2}{3} \right) \phi \right] \quad (16)$$

The equations ε_{Fz-U} and ε_{Fz-L} for calculating the strains on the upper surface and lower surface of the plate beam 5 can be derived into the following by substituting the above equations into the bending strain equation $\varepsilon = M_x / EZ_{2p}$ and the compression or the tension strain equation $\varepsilon = F / A_2(b_2l_2)E$

$$\begin{aligned} \varepsilon_{F_x-U} &= \frac{6t_2x}{l_2^3}(v + (a + \frac{l_2}{2})\phi) \\ &- \frac{6t_2}{l_2^2}(\frac{v}{2} + (\frac{a}{2} + \frac{l_2}{3})\phi) + \frac{d\phi}{l_2} \end{aligned} \quad (17-a)$$

$$\begin{aligned} \varepsilon_{F_x-L} &= -\frac{6t_2x}{l_2^3}(v + (a + \frac{l_2}{2})\phi) \\ &+ \frac{6t_2}{l_2^2}(\frac{v}{2} + (\frac{a}{2} + \frac{l_2}{3})\phi) - \frac{d\phi}{l_2} \end{aligned} \quad (17-b)$$

2.4 Design of sensing elements

The 3-axis force sensor for measuring the forces F_x , F_y and F_z should be designed in consideration of the design variables. Such as; the attachment location is respect to the size of the strain gauge, the rated capacity, the rated strain, the width b_1 and b_2 , the length l_1 and l_2 , the thickness t_1 and t_2 of the plate beams, the x -direction length from the contact plate to the end of plate beam a , the x -direction length between two plate beams of the PPB 5 d .

In order to design the sensing elements, the rated capacity of the F_x , F_y and the F_z sensors were determined be 100 N, respectively. The rated strains of the F_x sensor, the F_y sensor and the F_z sensor were approximately determined be $1000 \mu\text{m}/\text{m}$. The attaching locations of the strain gauges for the F_x sensor, the F_y sensor and the F_z sensor were determined be 2 mm from each end point of the plate beams in the length direction of the plate beams and at the central line in the width direction of the plate beams.

The size of each sensor was calculated by substituting the determined values into the derived strain equations (9-a), (9-b), (17-a) and (17-b). It showed that the width of plate beams $b_1 = b_2$ was 16 mm, the length of plate beams l_1 was 12 mm, l_2 was 10 mm, the thickness of plate beams t_1 was 1.46 mm, t_2 was 1.79 mm, a was 10 mm, d was 12 mm. The material of the plate beams is Al 2024-T351.

3. Finite element analysis

The sensing elements of each sensor are analyzed by using the FEM to confirm the strains calculated from the derived equations when the forces F_x , F_y and F_z are applied to each sensor. In doing this, the ANSYS

program was used. The strains on the surfaces of the plate beams are analyzed in three dimensions. To analyze the plate beams, the material constants of the beams require that the modulus of the longitudinal elasticity be 70 GPa and the poisson's ratio be 0.3. The plate beams have a mesh-size of 0.5 mm in the length direction, and the mesh size is trisected in the height direction. To analyze the plate beams of each sensor using the FEM analysis, the rated capacity of each sensor is applied to the beams of each sensor : the forces $F_x=F_y=F_z$ are 100 N.

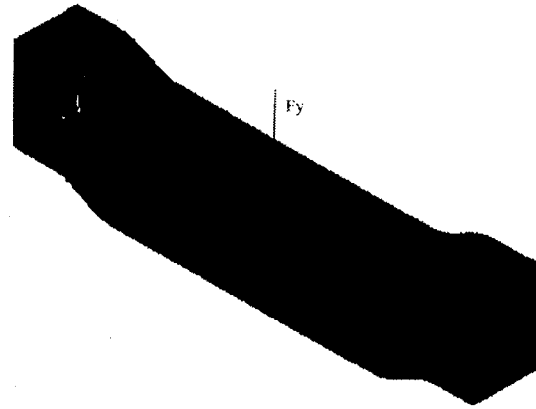


Fig. 6 Finite element mesh and deformed shape of beams for F_x or F_y force sensor under the force F_x or F_y

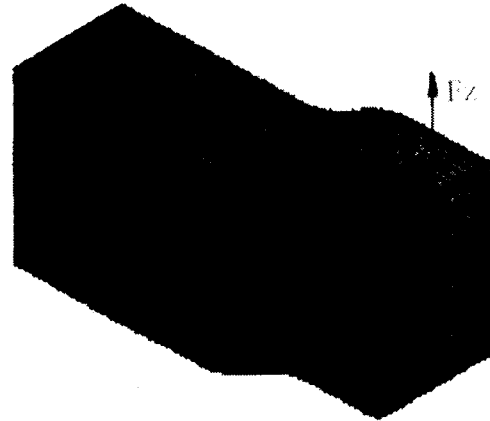


Fig. 7 Finite element mesh and deformed shape of beams for F_z force sensor under the force F_z

Fig. 6 and Fig. 7 show the deformed shape of the sensing elements for the F_y sensor and F_z sensor under force F_y and F_z , respectively. The deformed shape of the

sensing elements for the Fy sensor under the force Fy is symmetrical with respect to the vertical center axis. Also, the deformed shape of the sensing elements (upper and lower plate beams) for the Fz sensor under the force Fz shows similarity with respect to the horizontal center axis.

4. Results and Considerations

Fig. 8 shows the attachment locations of the strain gauges for each sensor. The locations of attachment of the strain gauges for each sensor are as follows: for the Fx sensor S1~S4, for the Fy sensor S5~S8 and for the Fz sensor S9~S12. The full bridge for each sensor is constructed by using the selected strain gauges for each sensor as shown in the Fig. 9. The rated strain and the interference strain are calculated using the equation

$$\varepsilon = \varepsilon_{T1} - \varepsilon_{C1} + \varepsilon_{T2} - \varepsilon_{C2} \quad (18)$$

where ε is the rated strain or the interference error, ε_{T1} is the strain from the tension strain gage T_1 , ε_{T2} is the strain from the tension strain gage T_2 , ε_{C1} is the strain from the compression strain gage C_1 , ε_{C2} is the strain from the compression strain gage C_2 .

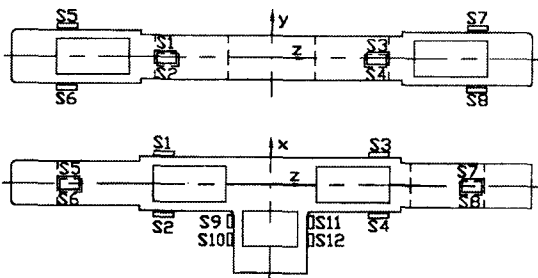


Fig. 8 Attachment locations of the strain gauges for each sensor

The strain gauges were attached at the selected attachment locations using a bond (M-bond 200, Micro-Measurement Company).

In order to reduce the interference error, the full bridge circuit for each sensor is constructed using strain gauges S1(C_1), S2(T_1), S3(C_2), S4(T_2) for the Fx sensor, S5(C_1), S6(T_1), S7(C_2), S8(T_2) for the Fy sensor and S9(T_1), S10(C_1), S11(T_2), S12(C_2) for the Fz sensor. Strain gauges (N2A-13-T001N-350, Micro-Measurement Company) were used for making the 3-axis force sensor.

The gage factor is 2.08, the length and the width are 1.52 mm and 2.54 mm, respectively. Fig. 10 shows the 3-axis force sensor developed.

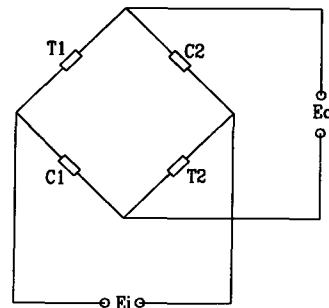


Fig. 9 Full bridge circuit

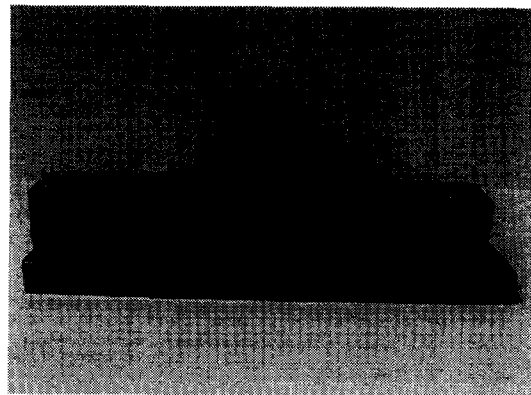


Fig. 10 3-axis force sensor developed

The 3-axis force sensor developed was calibrated using the 6-component force/moment sensor calibration machine¹². The forces Fx, Fy and Fz of 100 N (the rated capacity of the 3-axis force sensor) and the moments Mx, My and Mz of 0.5 Nm were applied to the 3-axis force sensor using the 6-component force/moment sensor calibration machine. This is because the interference errors may be generated from the Fx sensor, Fy sensor and Fz sensor under the moments Mx, My and Mz.

Table 1 shows the rated strains and the interference errors of each sensor from the theoretical analysis, the FEM and the experiment, and Table 2 shows the interference errors of each sensor in experiment. The rated strains of Fx sensor are 1000 $\mu m/m$ in the theoretical analysis, 987 $\mu m/m$ in the FEM and 961 $\mu m/m$ in the experiment. The rated strains of Fy sensor are 1000 $\mu m/m$ in the theoretical analysis, 987

$\mu m/m$ in the FEM and 1055 $\mu m/m$ in the experiment. The rated strains of Fz sensor are 1000 $\mu m/m$ in the theoretical analysis, 980 $\mu m/m$ in the FEM and 1048 $\mu m/m$ in the experiment.

Table 1 Rated strains and interference errors of each sensor

Force sensor	Analysis	Rated strain ($\mu m/m$)	Interference error (%)
Fx sensor	Theory	1000	0
	FEM	987	0
	Exper.	961	0.89
Fy sensor	Theory	1000	0
	FEM	987	0
	Exper.	1055	0.94
Fz sensor	Theory	1000	0
	FEM	980	0
	Exper.	1048	0.87

Table 2 Interference errors of each sensor in experiment

Sensor	Interference error (%)						Max.
	Fx=100 N	Fy=100N	Fz=100N	Mx=0.5 Nm	My=0.5 Nm	Mz=0.5 Nm	
Fx	-	0.11	0.23	0.37	0.89	0.15	0.89
Fy	0.13	-	0.43	0.94	0.15	0.04	0.94
Fz	0.76	0.87	-	0.37	0.21	0.55	0.87

Comparing the rated strain from the theoretical analysis with that of the FEM analysis, the rated strain errors are obtained as follows: less than 1.3 % for Fx, Fy sensors and 2.0 % for Fz sensor. This may have been caused due to the numerical error of the FEM software used for the finite element analysis. Also, comparing the rated strain from the theoretical analysis with that of the experiment, the rated strain errors are obtained as follows: less than 3.9 % for the Fx sensor, the 5.5 % for Fy sensor and 4.8 % for the Fz sensor. Thus, the maximum error of the rated strain is less than 5.5 %.

The interference errors of the 3-axis force sensor are as follows: for each sensor 0 % in the FEM and the theoretical analysis, for the Fx sensor, Fy sensor and Fz sensor 0.89 %, 0.94 % and 0.87 % in the experiment, respectively. Thus, the maximum error of the interference is less than 0.94 %. These errors may be generated due to the processing error, the error in

attachment of strain gages, the error in the characteristic test of the sensor, and so on.

5. Conclusions

This paper describes the design of robot's hand with two fingers for stably grasping an unknown object, and the development of the 3-axis force sensor for constructing a robot's finger. The robot's hand is composed of two fingers, two links, four motors and a block. The 3-axis force sensor was newly modeled by five PPBs, and fabricated. Comparing the rated strain from the theoretical analysis with that of the experiment, the maximum error of the rated strain is less than 5.5 %. Therefore, the derived strain equations ((9-a), (9-b), (17-a) and (17-b)) may be used for calculating the rated strains of the 3-axis force sensor developed in this study. The maximum error of the interference of the 3-axis force sensor is 0.94 % in the experiment. This is less than the 2~10% interference error found in other sensors for the robot's finger.

Acknowledgement

This work was supported by Engineering Research Institute in Gyeongsang National University.

References

1. Ceccarelli, M., et al., "Grasp Forces in Two-finger: Modeling and Measuring," Proceedings of 5th International Workshop on Robotics in Alpe Adria-Danube Region, pp. 321-326, 1996.
2. Castro, D., et al., "Tactile Force Control Feedback in Parallel Jaw Gripper," Proceedings of the IEEE International Symposium on Industrial Electronics, Vol. 3, V. 3, pp. 884-888, 1997.
3. Tlale, N. S., et al., "Intelligent Gripper using Low Cost Industrial," Proceedings of the IEEE International Symposium on Industrial Electronics, Vol. 2, V. 2, pp. 415-419, 1998.
4. Valente, C. M., et al., "BRF Competitive Hopfield Neural Networks for Objects Grasping," Proceedings of the Fourth International Conference on Motion and Vibration Control, Vol. 3, V. 3, pp. 1171-1176, 1998.

5. O'Brien, D. J., et al., "Force Explicit Slip Sensing for the Amadeus underwater Gripper," *International Journal of Systems Science*, Vol. 29 No. 5, pp. 471-483, 1998.
6. Yabuki, A., "Six-Axis Force/Torque Sensor for Assembly Robots," *FUJTSU Science Technology*, Vol. 26 No. 1, pp. 41-47, 1990.
7. Brussel, H. V., Belien, H. and Thielemans, H., "Force Sensing for Advanced Robot Control," *North-Holland Robotics2*, pp. 139-148, 1986.
8. Lee, J., "Apply Force/Torque Sensors to Robotic Applications," *North-Holland Robotics2*, pp. 139-148, 1987.
9. Hatamura, Y., et al., "A Miniature 6-axis Force Sensor of Multilayer Parallel Plate Structure," *IMEKO*, pp. 567-582, 1989.
10. Ono, K., et. al., "A New Design for 6-component Force/Torque Sensors," *Mechanical Problems in Measuring Force and Mass*, pp. 39-48, 1993.
11. Kim, G. S., et. al., "Design and Fabrication of a Three-Component Force/Moment Sensor using Plate-Beam," *Meas. Sci. Technol.*, Vol.10, pp. 295-301, 1999.
12. Kim, G. S., "The Development of a 6-axis Force/Moment Sensor Testing Machine and Evaluation of its Uncertainty," *Measurement Science and Technology*, Vol. 11, pp. 1377-1382, 2000.
13. Kim, G. S., "Design of 3-component Force/Moment Sensor with Ratio of Wide Range," *Korean Society of Precision Engineering*, Vol. 18, No. 2, pp. 214-221, 2001.